

Separating the Wheat from the Chaff: Bayesian Regularization in Dynamic Social Networks

Diana Karimova^a, Roger Th.A.J. Leenders^{b,c}, Joris Mulder^{a,b}

^a Department of Methodology and Statistics, Tilburg School of Social and Behavioral Sciences, Tilburg University

^b Jheronimus Academy of Data Science

^c Department of Organization Studies, Tilburg School of Social and Behavioral Sciences, Tilburg University

Corresponding author:

Diana Karimova

Email: d.karimova@uvt.nl

Work Address: Warandelaan 2, Tilburg, Netherlands, 5037 AB

Separating the Wheat from the Chaff: Bayesian Regularization in Dynamic Social Networks

Abstract

In recent years there has been an increasing interest in the use of relational event models for dynamic social network analysis. The basis of these models is the concept of an “event”, defined as a triplet of time, sender, and receiver of some social interaction. The key question that relational event models aim to answer is what drives social interactions among actors. Researchers often consider a very large number of predictors in their studies (including exogenous variables, endogenous network effects, and various interaction effects). The problem is however that employing an excessive number of effects may lead to model overfitting and inflated Type-I error rates. Consequently, the fitted model can easily become overly complex and the implied social interaction behavior becomes difficult to interpret. A potential solution to this problem is to apply Bayesian regularization using shrinkage priors. In this paper, we propose Bayesian regularization methods for relational event models using four different priors: a flat prior model with no shrinkage effect, a ridge estimator with a normal prior, a Bayesian lasso with a Laplace prior, and a horseshoe estimator with a numerically constructed prior that has an asymptote at zero. We develop and use these models for both an actor-oriented relational event model and a dyad-oriented relational event model. We show how to apply Bayesian regularization methods for these models and provide insights about which method works best and guidelines how to apply them in practice. Our results show that shrinkage priors can reduce Type-I errors while keeping reasonably high predictive performance and yielding parsimonious models to explain social network behavior.

Keywords: Bayesian regularization, shrinkage priors, Bayesian lasso, horseshoe prior, relational event data

1 Introduction

Relational event history data is becoming increasingly available, partly due to increased use of technology-supported interaction, such as email, phone calls, and online social networks (Twitter, Facebook, et cetera). Relational event data encode who does what with respect to whom at what point in time. Typically, relational event data contain information of the exact timing (or order) of interactions, who was the sender, who was the receiver, and, possibly, what was the mode of communication (e.g., face-to-face or digital), the sentiment (e.g., positive or negative), the content, et cetera. Additionally, information about attributes of the involved actors is also often available, for example gender, group memberships, or the hierarchical position of an actor. Finally, information about possible external influences to the event history, such as deadlines, the start of new projects, or time-of day/day-of-week effects in social networks in organizations, may be available. Thus, due to its high-resolution, relational event data can potentially greatly support our understanding of complex interaction processes, about temporal effects of interventions in networks, or about how past interactions may affect what will happen in the (nearby) future.

Relational event models (initially proposed by Butts (2008), and later extended by DuBois et al. (2013), Quintane et al. (2014), Leenders et al. (2016), Pilny et al. (2016), Vu et al. (2017), Stadtfeld et al. (2017), Mulder and Leenders (2019), Lerner and Lomi (2020), among others) have become widely used over the past decade for analyzing relational event data. In the relational event model, the outcome variable is the rate of interaction between potential senders and receivers in the network at a given time point. This rate of interaction is commonly assumed to be a log linear function of a set of predictor variables (at that given point in time). Following Leenders et al. (2016), predictor variables can be categorized as being endogenous (summarizing the past activity of the actors in the network) or exogenous (capturing actor attributes or external influences). Essentially, the relational event model aims to predict the next event: given the past interactions among the actors and the characteristics of the actors, at a given time t , what will be the next interaction (and when will it occur)? In relational event models, this is achieved by finding a loglinear combination of endogenous and exogenous predictors that best (or, sufficiently) model the rates of interaction of every event that is possible at t .

There are at least three ways in which researchers aim to build relational event models (and these approaches are also frequently applied in the fitting of other complex network models for which substantive theory is scant, such as (S)(T)ERGM's or SIENA-models). First, when researchers have a theory of what drives the social in-

teraction dynamics in a network, predictors are chosen to reflect the theory at hand. Unfortunately, there is almost no successful theory that explains who interacts with whom and at what rate (and who don't), so there is rarely a decent theoretical foundation for researchers to base the selection of predictors on. A second approach is to engage in a data mining-like approach by adding and removing predictors until the best achievable model has been reached. Typically, researchers start with a set of predictors (inspired by theory or previous findings), remove those that are not statistically significant and add new ones that might improve accuracy further, until the researcher is satisfied with the model fit. This is a potentially time-consuming approach that makes the interpretation of t -statistics highly questionable and disallows the model to be used for inferential purposes. A third approach is to throw a great many variables into the model and then interpret the signs and statistical significance of all of the predictors. This latter approach is statistically more acceptable, but the researcher runs the risk of including statistics that are highly mutually correlated and the resulting model may very well overfit the data. Although we are much in favor of the first approach, it is undermined by the dearth of solid theory to begin with. In an empirical project, the researcher therefore needs an approach to separate the wheat from the chaff in order to distinguish which predictors really matter and which do not. In statistics, this can be addressed using variable selection algorithms.

Variable selection algorithms have not yet been thoroughly developed for relational event models, but researchers have developed some ways to help the variable selection process. For example, Butts (2008) proposed a model for explaining radio communication messages between emergency transponders during the 9/11 World Trade Center disaster. To make decisions about which variables to include, Butts (2008) utilized the BIC, a model selection criterion that balances model fit and model complexity (via the number of predictor variables). In most cases, however, it is not computationally feasible to compute the BIC for all possible models since the more predictors are considered, the more models need to be fitted in order to compute all of the BIC's and find the model with the lowest BIC. Hence, in practice researchers only compare a few competing models. This choice of which models to compare is inherently arbitrary (to an extent) considering the aforementioned lack of solid theory to build on, and may be driven by computational burden (the longer it takes for a model to run, the fewer models can feasibly be compared).

Another possible solution for variable selection problems exists in a form of penalized or regularized regression. In penalized regression a penalty term is added to the sum of squared residuals. This results in shrinkage of small negligible effects (moving

them to zero) while leaving large effects largely unaffected. Therefore, small effects are removed from the model (as the coefficients end up close to zero and may lose statistical significance) and the effects that truly matter stay intact. The result is a more parsimonious model that highlights which effects really matter, without the “clutter” of many effects that do not contribute much statistically. Both frequentist and Bayesian regularization approaches have been shown to effectively guard against overfitting and to result in good predictive performance (Tibshirani, 1996; Park and Casella, 2008; Kyung et al., 2010; Van Erp et al., 2019). In this paper, we therefore contend that a useful and statistically sound alternative to the third approach above would be to specify a fairly large model (i.e. include all potential predictors of interest, regardless of multicollinearity) and then use regularization to separate the wheat from the chaff among all of the predictors at once.

In particular, we introduce a Bayesian regularization approach for relational event models. One of the benefits of Bayesian approach is that Bayesian regularization performs competitively and sometimes better than its classical counter parts (in terms of *predictive mean squared error*) and results in more accurate standard errors (via posterior standard deviations) (Park and Casella, 2008). Furthermore, a Bayesian approach is natural for regularization since the prior naturally serves as a penalty function. Bayesian approaches are not restricted to non-concave penalty functions that are computationally difficult to optimize in a maximum likelihood framework. Another advantage of the Bayesian approach is the possibility to fit all parameters of the model in one step, instead of using ad-hoc two-step methods where the penalty parameter needs to be separately determined, e.g., using cross-validation. In this paper, we will consider four different priors that each regularize relational event models differently. First, we will consider a flat prior to serve as a reference as it results in no shrinkage. This makes it comparable to ordinary maximum likelihood. Second, we consider Bayesian ridge regression using a Gaussian prior. Third, we develop Bayesian lasso regression using LaPlace priors (Park and Casella, 2008), which has thicker tails than the Gaussian prior and a higher peak at zero. Finally, we consider the (non-concave) horseshoe prior that is constructed via an F distribution. Originally proposed by Carvalho et al. (2010), the horseshoe prior has a spike at zero and thicker tails than a Cauchy distribution. We will discuss the implementation of these Bayesian regularization algorithms and illustrate their use for both a dyadic and an actor-oriented relational event model.

In Section 2 of this paper we explain two partial likelihood approaches to relational event modelling: one for a dyadic relational events and one for actor-oriented events. In Section 3 we discuss the four priors for Bayesian regularization, and in Section 4 we

illustrate the methodology with two empirical examples. We conclude and provide final discussions in Section 5.

2 Relational event modelling using partial likelihoods

The relational event model was popularized by Butts (2008), who modeled a relational event history as a Poisson process where the event rate for each specific dyad depends on a set of endogenous and exogenous effects through a loglinear function.

Instead of working with the full likelihood for a joint model for all event times, senders, and receivers, in this paper we adopt the idea of partial likelihoods (Cox, 1972; Perry and Wolfe, 2013) that only considers specific parts of a conditional likelihood. By working with partial likelihoods, we simplify the specification of the model by focusing on the outcome variables that are of most interest for a given application. Below, we first present a partial likelihood that is actor-oriented, was proposed by Perry and Wolfe (2013) and further developed by Stadtfeld et al. (2017). This approach may be preferred when a researcher is mainly interested in modeling the choice of the receiver of an event conditional on the sender (Vu et al., 2017; Stadtfeld and Block, 2017; Hoffman et al., 2020; Hedström and Bearman, 2009). Second, we provide a partial likelihood for a dyadic relational event model which has not yet been considered in the literature, to our knowledge. This latter approach may be preferred when one is interested in modeling the full dyad (sender and receiver jointly) (Leenders et al. (2016), Brandes et al. (2009), and numerous direct applications of REM, such as Malang et al. (2019), Liang (2014), Lerner and Lomi (2018).

2.1 Partial likelihood for an actor-oriented model

Using the notation of events $e_m = (t_m, s_m, r_m)$, $m \in \{1, \dots, M\}$ as a triplets of time t , sender s , and receiver r , we can write the likelihood of the sequence of events as a product of conditional likelihoods:

$$\begin{aligned}
 L(e_1, \dots, e_M) &= L(e_1)L(e_2, \dots, e_M) = L(e_1)L(e_2|e_1) \cdot \dots \cdot L(e_M|e_1, \dots, e_{M-1}) = \\
 &= L(t_1, s_1)L(r_1|t_1, s_1)L(t_2, s_2|t_1, s_1, r_1)L(r_2|t_2, s_2, e_1) \cdot \dots \cdot \\
 &\quad \cdot L(t_M, s_M|e_{M-1}, \dots, e_1)L(r_M|t_M, s_M, e_{M-1}, \dots, e_1)
 \end{aligned} \tag{1}$$

Without loss of generality, we can focus on the choice of the receiver, for a given point in time and a given sender. In most research projects, understanding who will be the receiver of an event is more informative than modeling who will be the sender. We thus consider the following partial likelihood of the receivers of the events conditional on the senders and event times, which follows directly from equation (1):

$$PL(\mathbf{r}|\mathbf{s}, \mathbf{t}) = L(r_1|t_1, s_1) \cdot L(r_2|t_2, s_2) \cdot \dots \cdot L(r_M|t_M, s_M) \quad (2)$$

The partial likelihood in (2) can be seen as a statistical choice model, where the sender “chooses” the most suitable receiver of an interaction from the set of possible receivers. In this paper we consider a Bayesian probit model using a Gaussian latent variable approach by extending the work of Imai and Van Dyk (2005) to relational data. For each event e_i in a sequence $\{e_1, \dots, e_M\}$, where M is a total number of events, we define a categorical outcome variable Y_i that represents a receiver of the event e_i . This receiver of event i can be any actor in the *risk set* \mathcal{R}_{actor} – the set of actors who are possible receivers of a given event. For simplicity, we assume that all actors, except for the sender, are at risk. In our latent variable approach the sender assigns a latent “suitability scale” to all potential receivers in the risk set. The latent suitability of actor r for a given sender s_i is denoted by Z_{ir} . The receiver r with the largest Z_{ir} will be the predicted receiver of the event:

$$Y_i(Z_i) = r, \text{ if } \max(Z_i) = Z_{ir}, \quad (3)$$

where $Z_i = (Z_{i1}, \dots, Z_{iN})$ is a multivariate latent variable. In the framework of the multivariate probit model, we can write

$$Z_i = X_i\boldsymbol{\beta} + \epsilon_i, \quad (4)$$

where X_i is a $N \times P$ matrix of observed predictor variables at time i , $\boldsymbol{\beta} = (\beta_1, \dots, \beta_P)^T$ is a vector of network parameters, and ϵ_i is a Gaussian error term, centered at zero, having an identity covariance matrix (to ensure identifiability of the model). The matrix $X_i, i = 1, \dots, M$ of predictor variables can include endogenous as well as exogenous predictors, defined for each actor in the risk set. Network effects that are calculated on a pair of sender and receiver are often not defined for loop events, when a sender and a receiver are the same actor. In such cases the corresponding row of matrix X_i is empty.

2.2 A partial likelihood for a dyadic model

In certain applications the interest is in jointly modeling the combination of sender and receiver (Leenders et al., 2016; Brandes et al., 2009; Malang et al., 2019; Liang, 2014; Lerner and Lomi, 2018). Thus, unlike the choice model of the receiver given the sender, we build a statistical model for all possible dyads that can be observed at a given point in time. Starting from the same full likelihood, but redefining the conditional likelihood in such a way that we condition on the time points of events, we get the following representation of the likelihood:

$$\begin{aligned}
 L(e_1, \dots, e_M) &= L(e_1)L(e_2, \dots, e_M) = L(e_1)L(e_2|e_1) \cdot \dots \cdot L(e_M|e_1, \dots, e_{M-1}) = \dots = \\
 &= L(t_1)L(s_1, r_1|t_1)L(t_2|t_1, s_1, r_1)L(s_2, r_2|t_2, e_1) \cdot \dots \cdot \\
 &\quad \cdot L(t_M|e_{M-1}, \dots, e_1)L(s_M, r_M|t_M, e_{M-1}, \dots, e_1)
 \end{aligned} \tag{5}$$

A partial likelihood for a dyad REM can be written as follows:

$$PL(\mathbf{s}, \mathbf{r}|\mathbf{t}) = L(s_1, r_1|t_1) \cdot L(s_2, r_2|t_2) \cdot \dots \cdot L(s_M, r_M|t_M) \tag{6}$$

This can be viewed as a dyadic partial likelihood for the REM where the sender and receiver for event e_i are jointly modeled.

In contrast with the previous model, in the dyadic model the outcome variable is the rate of a dyad. In particular, Y_i is defined as an index of the dyad (s, r) from the risk set \mathcal{R}_{dyad} of all the $N(N - 1)$ possible ordered dyads. Following the idea of a multivariate probit model, we assume that all dyads that are at risk lie on a “latent activity scale”; the dyad with the largest latent activity score becomes the dyad that is predicted to occur next:

$$Y_i(W_i) = l(s_i, r_i), \text{ if } \max(W_i) = l(s_i, r_i),$$

where $l(s_i, r_i) \in \{1, \dots, N(N - 1)\}$ is the index of dyad (s_i, r_i) in ordered risk set \mathcal{R}_{dyad} . Therefore, latent vectors W_i have length $N(N - 1)$, under the condition that an actor cannot send an event to oneself. Note that a long length of the latent variable can lead to a high computational cost for larger networks as there will be many unknown latent variables to be estimated.

We write the regression for the dyad REM as follows:

$$W_i = X_i\boldsymbol{\beta} + \epsilon_i, i = 1, \dots, M \tag{7}$$

where matrices X_i are of dimension $N(N - 1) \times P$ (containing the dyadic predictor variables) and $\boldsymbol{\beta}$ is the corresponding vector that quantifies the relative importance of the predictors. As in the actor-oriented model, the set of potentially important dyadic predictor variables can be huge. To find the true nonzero effects, a Bayesian regularization algorithm will be proposed, as discussed in the next section.

3 Bayesian regularization via shrinkage priors

The complete Bayesian model combines the statistical model for the data with a prior distribution for the network parameters $\boldsymbol{\beta}$ ¹:

$$\begin{aligned} \text{model} & : \begin{cases} Y_i(Z_i) & = j, \text{ if } \max(Z_i) = Z_{ij}, \\ Z_i & = X_i\boldsymbol{\beta} + \epsilon_i, \text{ with } \epsilon_i \sim N(0, I) \end{cases} \\ \text{prior} & : p(\boldsymbol{\beta}) \end{aligned}$$

In many applications of Bayesian statistical methods, the prior is used to add external information to the analysis, e.g., reflecting expert knowledge or previous empirical findings. In Bayesian regularization, on the other hand, the prior acts as a penalty function that shrinks negligible effects towards zero while leaving large effects mostly unaffected. This is why the priors in these models are often referred to as “shrinkage priors.” The result of this behavior is that the resulting model is more parsimonious than the unregularized model, showing which variables matter a lot and which might as well be neglected. To allow the same type of shrinkage behaviour for negative and positive effects, the prior should have a symmetric form with a peak at zero (to shrink small effects) while having some probability mass allocated in the tails (to leave large effects largely unaffected).

Different types of priors can be used for this purpose. For a recent overview, see Van Erp et al. (2019). In the current paper, we consider three of the most popular shrinkage priors from the Bayesian regularization literature: a Gaussian prior (for Bayesian ridge regression), a LaPlace prior (for Bayesian lasso regression), and a horse-shoe prior. Figure 1 displays these priors. We add a flat (horizontal) improper prior

¹In this section we describe the priors in the case of actor-oriented model. The priors for the dyadic model are mathematically equivalent to the ones described in sections 3.1, 3.2, 3.3, 3.4.

that does not perform any shrinkage (as it assumes that all values of the parameters are equally likely a priori). The results of the flat prior are comparable with maximum likelihood estimation, making it a perfect reference.

The variance of a shrinkage prior has a direct effect on the amount of shrinkage in the model: a large (small) prior variance induces little (considerable) shrinkage. This prior variance is controlled via the *shrinkage parameter* and is denoted as λ^2 . Ideally, when there are many large effects, the shrinkage parameter should be large (so the large effects are left intact), and when there are hardly any large effects, the shrinkage parameter should be small (so the small effects are nudged towards zero). The optimal value of the shrinkage parameter for a given data set can be found using two-step approaches such as cross-validation or empirical Bayes methods (e.g., Park and Casella, 2008). A more natural choice is to estimate the shrinkage parameter jointly with the Bayesian model in one step, yielding a full Bayesian model. This only requires one to specify a separate prior density for the shrinkage parameter λ^2 .

To fit the Bayesian regularized relational event models, we use Markov Chain Monte Carlo (MCMC) methods to sample the parameters from the joint posterior. The approach is to sample the model parameters sequentially from their conditional posterior distributions. Gibbs sampling is a specific MCMC algorithm where the conditional posterior distributions of the parameters belong to known distributional families from which it is easy to sample. This is generally the case when the priors have the same distributional form as the likelihood (this is known as “conjugacy”). Because of the Gaussian errors of the latent variables in the partial likelihoods from Section 2, Gaussian priors for β result in conditional posteriors that also have Gaussian distributions. It is possible to write the Bayesian lasso prior and the horseshoe prior conditionally as scaled mixture of Gaussian priors, to ensure easy and efficient posterior sampling using Gaussian posteriors. For the shrinkage parameters, we consider F priors as they are relatively vague while allowing easy posterior sampling using Gamma and Inverse distributions (Mulder et al., 2018). This is equivalent to choosing a half-Cauchy prior for λ , which is a common choice (Carvalho et al., 2009). In the next section, we discuss each Bayesian shrinkage model for relational event analysis in detail.

3.1 Flat prior (no shrinkage)

We first consider a benchmark model with no shrinkage effect. This model utilizes a flat improper prior that assumes that all values for the regression coefficients vector

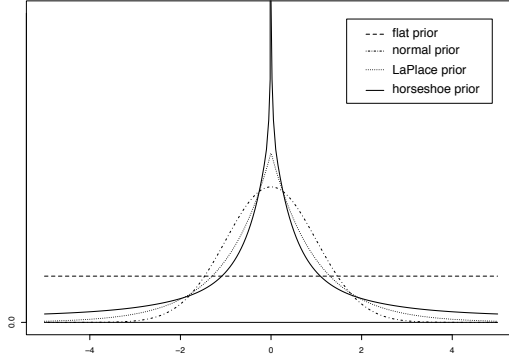


Figure 1: Flat prior (dashed line), normal prior (dash-dotted line), LaPlace prior (dotted line), and horseshoe prior (solid line).

$\boldsymbol{\beta} = (\beta_1, \dots, \beta_P)$ are equally likely a priori. Mathematically, this can be written as

$$p^{FLAT}(\boldsymbol{\beta}) \propto 1, \quad (8)$$

The prior density is constant over the complete real line (see the dashed line in figure 1). The prior does not shrink the regression coefficients: the estimates of the $\boldsymbol{\beta}$ will be entirely driven by the data. The Bayesian flat prior model, therefore, behaves very similar to classical MLE estimation. Given an observed event history we can estimate the posterior distribution of $\boldsymbol{\beta} = (\beta_1, \dots, \beta_P)$. Because the latent variable has a multivariate normal distribution, the model can be estimated using a Gibbs sampler that can be written as:

1. Set initial values for $\boldsymbol{\beta}^{(0)}$, and $Z^{(0)}$.
2. Given $Z^{(s-1)}$, draw $\boldsymbol{\beta}^{(s)}$ from its conditional posterior distribution that follows the multivariate normal distribution:

$$\boldsymbol{\beta}^{(s)} | Z^{(s-1)} \sim N(\mu_\beta, \Sigma_\beta), \text{ where}$$

$$\mu_\beta = \left(\sum_{i=1}^M X_i^T X_i \right)^{-1} \sum_{i=1}^M X_i^T Z_i^{(s-1)}, \quad \Sigma_\beta = \left(\sum_{i=1}^M X_i^T X_i \right)^{-1}$$

3. Given $\boldsymbol{\beta}^{(s)}$, draw $Z_{i_r}^{(s)}$ from its conditional posterior distribution that follows the truncated normal distribution:

$$Z_i^{(s)} | \boldsymbol{\beta}^{(s)} \sim t\mathcal{N}(X_i \boldsymbol{\beta}^{(s)}, I_N).$$

To reduce the degrees of freedom when choosing the latent variables, the first component of each Z_i is fixed to zero. The value of the element of Z_i that corresponds to the observed actor is generated from a truncated density on the interval $(\max_{r \neq r_i} Z_{ir}, \infty)$. Alternatively, the values of the elements that correspond to actors that are not observed are generated from the truncated density on the opposite interval $(-\infty, Z_{ir_i})$. This way we can guarantee that latent variables resemble the given relational event data.

4. Repeat steps 2 and 3 for $s = 1, \dots, S$.

The initial set of draws is discarded as they are part of the burn-in period and would depend on the arbitrarily chosen initial values. The remainder is used to construct Bayesian credible intervals, or point estimates such as posterior mode, for each β_1, \dots, β_P . These intervals indicate whether the data suggest that the effect is negligible or not.

3.2 Bayesian ridge prior

Ridge regression was originally developed to improve estimates of the classic least squares model, especially in the case when there is a high correlation among predictors. The model utilizes a modified variance matrix $X'X + \lambda^2 I$ that adds a quadratic penalty. In Bayesian ridge regression, a normal prior is used for the regression coefficients:

$$p^{RIDGE}(\boldsymbol{\beta} | \lambda^2) = \prod_{p=1}^P p(\beta_p | \lambda^2) = \prod_{p=1}^P \mathcal{N}(\beta_p | 0, \lambda^2), \quad (9)$$

where $\mathcal{N}(\beta_p | 0, \lambda^2)$ denotes a normal prior for β_p with mean 0 and variance λ^2 .

We plot this prior in Figure 1 using a dash-dotted line. The prior is centered around zero with relatively thin tails. Shrinkage is performed over the entire domain of parameters due to the structure of normal prior density: large values will be shrunk to the same degree as are small values.

To complete the Bayesian model, we need a prior for the shrinkage parameter λ^2 . A common prior for this purpose is the gamma distribution (Park and Casella (2008)). However, the hyperparameters of the gamma prior may considerably affect its results (Kyung et al., 2010). For this reason, we use a half-Cauchy prior for λ instead, which is quite vague due to its thick tails. A half-Cauchy prior for λ is equivalent to a matrix- F

prior for λ^2 (e.g., Mulder et al., 2018), which has density:

$$F(\lambda^2; \alpha_1, \alpha_2, b) = \frac{\Gamma(\frac{\alpha_1 + \alpha_2}{2})}{\Gamma(\frac{\alpha_1}{2})\Gamma(\frac{\alpha_2}{2})} b^{-\alpha_2/2} \left(\frac{\lambda^2}{b} + 1\right)^{-\frac{\alpha_1 + \alpha_2}{2}} (\lambda^2)^{\alpha_2/2 - 1} \quad (10)$$

The hyperparameters will be set to 1, which is the default minimally informative choice:

$$\lambda^2 \sim F(1, 1, 1)$$

Using a parameter expansion, the matrix- F distribution can be written as a scale mixture of inverse gamma distributions via

$$F(\lambda^2 | \alpha_1, \alpha_2, b) = \int IG(\lambda^2 | \frac{\alpha_2}{2}, \delta) G(\delta | \frac{\alpha_1}{2}, b) d\psi^2.$$

This makes the prior conditionally conjugate, which makes the MCMC algorithm quite efficient. The Gibbs Sampler algorithm is as follows:

1. Set initial values for $\beta^{(0)}$, and $Z^{(0)}$, as well as for parameters $\lambda^{2(0)}$, $\delta^{(0)}$.
2. Draw $\beta^{(s)}$ from its conditional posterior distribution given $Z^{(s-1)}$,

$$\beta^{(s)} | Z^{(s-1)} \sim \mathcal{N}(\mu^{ridge}, \Sigma^{ridge}), \text{ where}$$

$$\mu^{ridge} = \left(\sum_{i=1}^M X_i^T X_i + \frac{1}{\lambda^2} I_P \right)^{-1} \sum_{i=1}^M X_i^T Z_i^{(s-1)}$$

$$\Sigma^{ridge} = \left(\sum_{i=1}^M X_i^T X_i + \frac{1}{\lambda^{2(s-1)}} I_P \right)^{-1}$$

3. Draw $Z_{i_r}^{(s)}$ from its conditional posterior given $\beta^{(s)}$, which is a truncated normal distribution.

$$Z^{(s)} | \beta^{(s)} \sim t\mathcal{N}(X_i \beta^{(s)}, I_N)$$

To ensure that the sampled values of the latent variables correspond to the given data and satisfy equation (3), we sample latent variables in the following way: first element of each vector Z_i is set to zero to reduce degrees of freedom; the element that corresponds to the observed actor is sampled from a truncated normal density

on the interval $(\max_{r \neq r_i} Z_{ir}, \infty)$; and the elements which correspond to non-observed actors are sampled from truncated density on the complement interval $(-\infty, Z_{ir_i})$.

4. Draw the shrinkage parameter λ^2 and the expanded parameter δ :

$$\lambda^{2(s)} | \boldsymbol{\beta}^{(s)}, \delta^{(s-1)} \sim \text{IG}(\alpha_1 + \frac{P}{2}, \delta^{(s-1)} + \frac{1}{2} \sum_{p=1}^P (\beta_p^{(s)})^2)$$

$$\delta^{(s)} | \lambda^{2(s)} \sim \text{G}(\alpha_1 + \alpha_2, \frac{1}{\lambda^{2(s)}} + \frac{1}{b})$$

5. Repeat steps 2 to 4 for $s = 1, \dots, S$.

After discarding the initial set of draws as a burn-in period, the remainder is used to construct Bayesian credibility intervals.

3.3 Bayesian lasso prior

The classical lasso (“least absolute shrinkage and selection operator”) regression model uses a L_1 norm as a penalty term, which is the sum of the absolute values of the regression coefficients. The Bayesian equivalent of the lasso penalty is obtained by using a Laplace prior for regression coefficients (Park and Casella (2008)).

$$p^{LASSO}(\boldsymbol{\beta} | \lambda^2) = \prod_{p=1}^P \text{Laplace}(\beta_p | \lambda^2), \quad (11)$$

for $p = 1, \dots, P$. To facilitate Bayesian computation, the Laplace prior can be written as a normal distribution where the scale has an exponential distribution; this results in a conditionally conjugate Bayesian model:

$$\text{Laplace}(\beta_p | \lambda^2) = \int \mathcal{N}(\beta_p | 0, \tau_p^2 \lambda^2) \text{Exp}(\tau_p^2 | 1) d\tau_p.$$

We plot the Laplace prior as a dotted line in Figure 1; it is more peaked around zero compared to the normal (ridge) prior. In opposite to the ridge model estimates, this results in stronger shrinkage for small estimated effects and, due to the Laplace having thicker tails than the normal prior, less shrinkage for larger estimated effects.

Compared to the normal (ridge) prior, the lasso prior includes the parameter τ_p^2 ; this serves as a shrinkage parameter on a local level for effect β_p and varies across the β_p . The λ^2 parameter, on the other hand, controls global shrinkage and affects all β_p

to the same degree. The idea of a separate global and a local shrinkage parameter was introduced by Carvalho et al. (2009) and allows a researcher to control the shrinkage behavior of the method precisely. To complete the model, we set a vague matrix- F prior for the global shrinkage parameter:

$$\lambda^2 \sim F(1, 1, 1).$$

The steps in the Gibbs sampler are the following:

1. Set initial values for $\beta^{(0)}, Z^{(0)}, \lambda^{2(0)}, \tau_1^{2(0)}, \dots, \tau_P^{2(0)}, \delta^{(0)}$
2. Draw $\beta^{(s)}$ from its conditional posterior distribution given $Z^{(s-1)}, \tau_1^{2(s-1)}, \dots, \tau_P^{2(s-1)}, \lambda^{2(s-1)}$

$$\beta^{(s)} | Z^{(s-1)}, \tau_1^{2(s-1)}, \dots, \tau_P^{2(s-1)}, \lambda^{2(s-1)} \sim \mathcal{N}(\mu^{lasso}, \Sigma^{lasso}), \text{ where}$$

$$\mu^{lasso} = \left(\sum_{i=1}^M X_i^T X_i + D_\tau^{-1} \right)^{-1} \sum_{i=1}^M X_i^T Z_i^{(s-1)}$$

$$\Sigma^{lasso} = \left(\sum_{i=1}^M X_i^T X_i + D_\tau^{-1} \right)^{-1},$$

$$D_\tau = \text{diag}\{\lambda^{2(s-1)}\tau_1^{2(s-1)}, \dots, \lambda^{2(s-1)}\tau_P^{2(s-1)}\}$$

3. Update latent variables by sampling $Z_{ir}^{(s)}$ from its conditional posterior given $\beta^{(s)}$, which is a truncated normal distribution, such that

$$Z^{(s)} | \beta^{(s)} \sim t\mathcal{N}(X_i \beta^{(s)}, I_N).$$

and for an element of Z_i that corresponds to the observed actor the truncated interval is $(\max_{r \neq r_i} Z_{ir}, \infty)$ while elements that conform the actors that are not observed are truncated in the interval $(-\infty, Z_{ir_i})$. These conditions will guarantee that sampled latent variables fit the observed categorical data and according to equation (3). In addition, the first element of each Z_i is fixed to zero, such that there are less degrees of freedom in the generating process.

4. Draw the value of parameter $\tau^{2(s)} = (\tau_1^{2(s)}, \dots, \tau_P^{2(s)})$ from its conditional posterior distribution, which in this case is an inverse-Gaussian distribution:

$$\frac{1}{\tau_p^{2(s)}} |\beta_p^{(s-1)}, \lambda^{2(s-1)} \sim \text{Inv-Gauss}(\mu' = \sqrt{\frac{\lambda^{2(s-1)}}{\beta_p^{2(s-1)}}}, \lambda' = 1), p = 1, \dots, P$$

5. Update the values of $\lambda^{2(s)}$ (similarly to the step 4 for the ridge model):

$$\lambda^{2(s)} | \tau_1^{2(s-1)}, \dots, \tau_P^{2(s-1)}, \delta^{(s-1)} \sim IG(\alpha_1 + \frac{P}{2}, \delta + \frac{1}{2} \sum_{p=1}^P \frac{\beta_p^2}{\tau_p^2})$$

$$p(\delta^{(s)} | \lambda^{2(s-1)}) \propto G(\alpha_1 + \alpha_2, \frac{1}{\lambda^{2(s-1)}} + \frac{1}{b})$$

6. Repeat steps 2 to 5 for $s = 1, \dots, S$.

After discarding the burnin period, the posterior draws can be used to obtain posterior estimates and construct Bayesian credibility intervals.

3.4 Bayesian horseshoe prior

The horseshoe model was first introduced in Carvalho et al. (2010) and has the key shape characteristics of an asymptote at zero and heavier tails. To construct this prior, the original model proposes to use a half-Cauchy distribution (i.e., a Student t distribution with 1 degree of freedom). This results in heavier shrinkage of small effects and less shrinkage of large effects compared to the Bayesian lasso. The prior can be written as follows:

$$p^{HORSESHOE}(\beta | \lambda^2) = \prod_{p=1}^P \text{Horseshoe}(\beta_p | \lambda^2), \quad (12)$$

where λ^2 is a global shrinkage parameter. Again, to facilitate Bayesian computation the horseshoe prior can be written as a scaled mixture of normals where λ^2 follows a matrix- F distribution (which is equivalent with a half-Cauchy prior for λ), i.e.,

$$\text{Horseshoe}(\beta_p | \lambda^2) = \int \mathcal{N}(\beta_p | 0, \lambda^2 \tau_p^2) F(\tau_p^2 | 1, 1, 1) d\tau_p^2.$$

A graphical representation of the horseshoe prior is given in Figure 1 by the solid line. As can be seen the prior has a sharp peak at zero and heavy tails. The name “horseshoe” comes from the observation that the shrinkage coefficient κ_p , defined as $\kappa_p = 1/(1 + \tau_p^2)$, has a horseshoe-shaped $Beta(1/2, 1/2)$ distribution under the matrix- F prior for τ_p . This coefficient reflects the amount of weight that the posterior places

around zero: $\kappa_p \approx 0$ corresponds to no shrinkage whereas $\kappa_p \approx 1$ corresponds to total shrinkage to zero.

Similar to the Bayesian lasso prior, τ_p^2 serves as a local shrinkage parameter for β_p , while λ^2 serves as a global shrinkage parameter. In contrast to the Bayesian lasso, the local shrinkage parameters now follows an F distribution instead of an exponential distribution. As the F distribution has thicker tails than the exponential in case of Bayesian lasso, the F prior will result in less shrinkage of large effects than the lasso model. The parameter λ^2 optimizes the overall level of sparsity, while the local shrinkage parameters τ_p^2 prevent large effects from being shrunk towards zero. Again, we finalize the Bayesian horseshoe model by setting a vague F prior on the global shrinkage parameter:

$$\lambda^2 \sim F(1, 1, 1).$$

The model can be fitted efficiently using a Gibbs sampler algorithm with the following steps:

1. Set initial values for $\beta^{(0)}, Z^{(0)}, \boldsymbol{\lambda}^{2(0)} = (\tau_1^{2(0)}, \dots, \tau_P^{2(0)})$, $\lambda^{2(0)}$, and mixing parameters of the F densities: $\boldsymbol{\psi}^{2(0)} = (\psi_1^{2(0)}, \dots, \psi_P^{2(0)})$, $\gamma^{2(0)}$.
2. Draw $\beta^{(s)}$ from its conditional posterior distribution given $Z^{(s-1)}, \boldsymbol{\tau}^{2(s-1)}, \lambda^{2(s-1)}$

$$\beta^{(s)} | Z^{(s-1)}, \boldsymbol{\tau}^{2(s-1)}, \lambda^{2(s)} \sim \mathcal{N}(\mu^{horseshoe}, \Sigma^{horseshoe}), \text{ where}$$

$$\mu^{horseshoe} = \left(\sum_{i=1}^M X_i^T X_i + D_\tau^{-1} \right)^{-1} \sum_{i=1}^M X_i^T Z_i^{(s-1)}$$

$$\Sigma^{horseshoe} = \left(\sum_{i=1}^M X_i^T X_i + D_\tau^{-1} \right)^{-1},$$

$$D_\tau = \text{diag}\{\lambda^{2(s-1)}\tau_1^{2(s-1)}, \dots, \lambda^{2(s-1)}\tau_P^{2(s-1)}\}$$

3. Draw the values of latent variables by sampling $Z_{ir}^{(s)}$ from conditional posterior given $\beta^{(s)}$, which is a truncated normal distribution

$$Z^{(s)} | \beta^{(s)} \sim t\mathcal{N}(X_i \beta^{(s)}, I_N).$$

under the conditions that for an observed element of Z_i the truncated interval is

$(\max_{r \neq r_i} Z_{ir}, \infty)$ and for elements that are not observed the truncated interval is $(-\infty, Z_{ir_i})$, while the first element of Z_i is always set to zero. Such conditions form latent variables that correspond to the observed categorical data by the the definition of equation (3).

4. Draw the value of parameter $\boldsymbol{\tau}^{2(s)}$ from its conditional posterior - inverse gamma distribution

$$\tau_p^{2(s)} | \psi_p^{2(s-1)}, \lambda^{2(s-1)}, \beta_p^{(s)} \sim \text{IG} \left(\alpha_3 + \frac{1}{2}, \psi_p^{2(s-1)} + \frac{\beta_p^{2(s)}}{2\lambda^{2(s-1)}} \right), p = 1, \dots, P$$

5. Draw the value of parameter $\lambda^{2(s)}$ from its conditional posterior - inverse gamma distribution

$$\lambda^{2(s)} | \gamma^{2(s-1)}, \boldsymbol{\tau}^{2(s)}, \boldsymbol{\beta}^{(s)} \sim \text{IG} \left(\alpha_1 + \frac{P}{2}, \gamma^{2(s-1)} + \frac{1}{2} \sum_{p=1}^P \frac{\beta_p^{2(s)}}{\tau_p^{2(s)}} \right)$$

6. Update the mixing parameters $\boldsymbol{\psi}^{2(s)}$ and $\gamma^{2(s)}$:

$$\gamma^{2(s)} | \lambda^{2(s)} \sim \text{G} \left(\alpha_1 + \alpha_2, \frac{1}{b_1} + \frac{1}{\lambda^{2(s)}} \right)$$

$$\psi_p^{s(s)} | \tau_p^{2(s)} \sim \text{G} \left(\alpha_3 + \alpha_4, \frac{1}{b_2} + \frac{1}{\tau_p^{2(s)}} \right), p = 1, \dots, P$$

7. Repeat steps 2 to 6 for $s = 1, \dots, S$.

3.5 Comparison of priors in a simple hypothetical case

In order to illustrate the shrinkage effect of the four models we estimate the shrinkage models on relational event sequences of fixed length across increasing effect sizes. For this illustration we consider the actor-oriented model (but the shrinkage behavior is similar for the dyadic model). We create event sequences with different effect sizes by properly specifying the design matrix X. For example, consider a sequence of 30 relational events on a network of six actors, assuming a scalar network parameter β and a single predictor variable that is zero for all actors except for actor 2 (for whom it is equal to 0.2) for all events in the sequence ($i \in \{1, \dots, 30\}$):

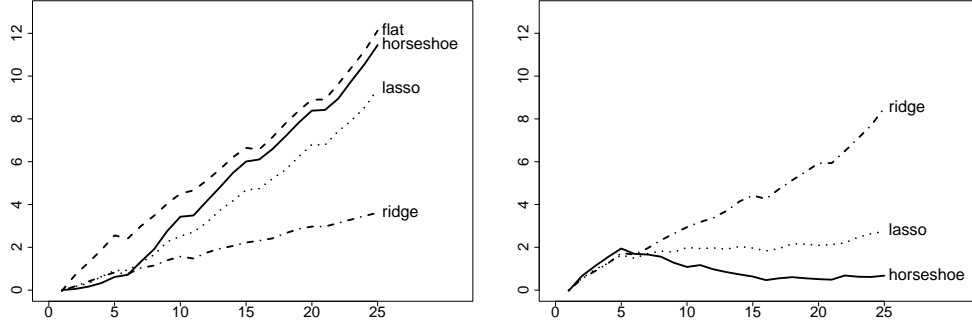
Event index	Sending actor	Receiver Sequence 1	Receiver Sequence 2	Receiver Sequence 3	...	Receiver Sequence 29
1	1	2	2	2		2
2	1	3	2	2		2
3	1	4	4	2		2
4	1	5	5	5		2
5	1	6	6	6		2
6	1	2	2	2		2
7	1	3	3	3		2
8	1	4	4	4		2
9	1	5	5	5		2
10	1	6	6	6		2
⋮	⋮	⋮	⋮	⋮		⋮
29	1	5	5	5		2
30	1	6	6	6		6

Table 1: Sequences of events with the allocation of the receivers. All senders are fixed to Actor 1. Receivers in Sequence 1 are distributed equally, in Sequence 29 all the receivers are Actor 2.

$$X_i = \begin{pmatrix} 0 \\ 0.2 \\ 0 \\ 0 \\ 0 \\ 0 \end{pmatrix}$$

Without the loss of generality, we assume that Actor 1 is the sender of all events. The number of actors who receive an event from actor 1 decreases across the sequences as shown in Table 1. In Sequence 1 all events are sent proportionally to all actors 2,3,..., 6. In the last Sequence 29 all events but one (to avoid identification issues) are sent to actor 2.

By construction, in these relational event sequences the effect size of β is smallest for the Sequence 1, grows gradually, and reaches its maximum for the Sequence 29. This data structure allows a clear comparison of the different shrinkage priors. The objective of this example is to check the amount and the shape of the shrinkage that the ridge, lasso, and horseshoe priors impose on a network effect. To see the clearest behaviors,



(a) Estimated coefficient for the flat, (b) Estimated difference between the ridge, lasso, and horseshoe models shrinkage models and the flat model

Figure 2: Estimated $\hat{\beta}$ for each generated sequence for the flat model (dashed line), ridge (dash-dotted line), lasso (dotted line), and horseshoe(solid line)

we fix the shrinkage parameter λ^2 to 1 for all models.

We used the actor oriented models to estimate the network effect for each of the 29 relational event sequences and show the resulting posterior means in Figure 2. The left panel shows the estimate $\hat{\beta}$ across Sequences 1 to 29 and the right panel shows the difference between the estimate under the flat prior with the estimate under each shrinkage model. The estimate based on the flat prior model, which serves as a reference, correctly increases over the sequence index. The ridge model shows an approximate linear trend, heavily shrinking moderate to large effects. The lasso model shrinks small effects a bit more than the ridge prior and yields estimates that are approximately parallel those of the flat model. The horseshoe shows most shrinkage for small effect sizes and the least shrinkage for larger effects where it gradually converges to the flat prior model. Next, we explore how the shrinkage prior models perform in empirical settings.

4 Empirical data applications

In this section we apply the Bayesian regularization algorithms to two empirical datasets. First we consider a relational event sequence based on the Enron corporate email data: the choice of the next receiver in this relational event sequence is analyzed using the actor-oriented models with shrinkage priors. Second, we consider a sequence of the communication messages from the famous Apollo 13 mission to the moon. This data is analyzed using the dyadic relational event models, in which the next dyad is pre-

dicted. The estimation is performed via R code which is available at (github page link suppressed for blind review). The purpose of these empirical examples is to show that the shrinkage models (i) result in fewer significant coefficients compared to the flat no shrinkage prior model, and thus provide a more parsimonious description of the interaction behavior in the networks, and (ii) have comparable, and in some cases improved predictive power.

The evaluation of the model performance is assessed via the posterior predictive distribution (Gelman et al. (2013)). In contrast to parametric bootstrapping (which only uses the MLE to predict observations), posterior predictive checks make use of the complete posterior of the parameters and thus take the uncertainty of the model parameters into account as well. Using the posterior predictive distribution, we can evaluate the performance of the fitted model by comparing the events predicted by the model with the events that actually occurred. Based on the posterior distribution, we can construct credible intervals and evaluate the significance of the particular effect by checking whether that interval covers zero. Additionally, to obtain point estimates we can look at the posterior mode of the effects based on the sample from conditional posterior densities.

To evaluate the predictive power of each model we use the latent variables $Z_i^{draw} = X_i\beta^{draw}$ that are calculated on the sampled values β^{draw} generated by the Gibbs sampler. Each component of the vector Z_i^{draw} corresponds to an actor from the ordered risk set. Higher values imply a larger probability of a corresponding actor to be the next receiver (or the dyad to transpire next in the case of dyad oriented model). Thus, we can compare the observed event with the set of “best predicted events”, i.e. sorted values of latent variable Z_i^{draw} , for any event in the sequence $e_i, i \in 1, \dots, M$. Below, we consider how often events with the highest Z_i^{draw} component are strictly equal to the observed event and how often it is in the set of 5%, 10%, or 20% of the highest scored events. This measure can be calculated for both in-sample or out-of-sample predictions.

4.1 Analyzing email data using the actor-oriented model

To demonstrate the performance of the actor oriented shrinkage models we used a publicly available data of the Enron corpus from the repository of Carnegie Mellon University. This dataset contains the time-stamped emails of 156 users, mostly senior management of Enron Corporation, a former American energy, commodities, and services company. The data were made public in 2001 after Enron Corporation declared bankruptcy and the following public investigation. It serves as a real life example of human communication, has been widely used in different fields, from social network re-

Variable	Characteristics of actor i
L(i)	member of the Legal department
T(i)	member of the Trading department
J(i)	seniority is Junior
F(i)	gender is Female

Table 2: Dichotomous variables indicating whether the actor works in the Legal department, trading department, is a junior, or is female.

search to computer science (Keila and Skillicorn, 2005; Diesner et al., 2005; Zhou et al., 2007; Wilson and Banzhaf, 2009; Peterson et al., 2011), and has already been analyzed in the context of relational events in Perry and Wolfe (2013) using maximum likelihood estimation with no shrinkage.

Exogenous actor traits available in the data describe the actors’ gender, department, seniority, job title, and company’s division. We include interaction variables as $X(i) * Y(i)$, where X and Y come from the set of dichotomous actor dependent attributes (L, T, J, F) – see Table 2 for the overview. We also included dichotomous statistics describing whether sender and receiver have the same job title (1= yes, 0 = no) whether they belong to the same division (1= yes, 0 = no).

As endogenous network effects, we include inertia and reciprocity – statistics that are commonly included in the analysis of relational event data (Leenders et al. (2016)). The inertia statistic of the event $e_m = (t_m, s_m, r_m)$ measures the number of events sent from actor s_m to actor r_m until time t_m . The reciprocity statistic measures the number of events sent from actor r_m to actor s_m until time t_m . Perry and Wolfe (2013) used interval-measured network effects to measure time dependence (see also Arena et al. (2021) for a memory decay models for relational event data). In this paper we adjusted time intervals to fit the chosen subset of events and calculated inertia and reciprocity on the intervals of 30 minutes, 1 hour, 2 hours, and 8 hours. The full list of effects used in the models is shown on Table 3.

We estimated the four models on a subset of 1000 first events² using the Gibbs sampler algorithms described in Section 2 with 10000 iterations as a burn-in period followed by a total of 100000 iterations, where only every tenth iteration is recorded (due to eliminate the effect of autocorrelation in the posterior draws). The estimated

²Relational event models make the implicit assumption that effects are constant over the included event sequence. If effects change during the event sequence (e.g., when a new project is started or when a vacation period starts), the parameter estimates no longer meaningfully capture the interaction reality and predictive accuracy of the relational event model may decrease strongly (Mulder and Leenders, 2019). Hence, we consider an event sequence that is short enough to reasonably assume stability of effects.

Effect	Description
Endogenous dyadic effects	
Inertia 1	Inertia on the interval of less than 30 minutes
Inertia 2	Inertia on the interval from 30 minutes to 1.1 hours
Inertia 3	Inertia on the interval from 1.1 hours to 2 hours
Inertia 4	Inertia on the interval from 2 hours to 8 hours
Reciprocity 1	Reciprocity on the interval of less than 30 minutes
Reciprocity 2	Reciprocity on the interval from 30 minutes to 1.1 hours
Reciprocity 3	Reciprocity on the interval from 1.1 hours to 2 hours
Reciprocity 4	Reciprocity on the interval from 2 hours to 8 hours
Exogenous dyadic effects	
Ex1 = L(i)*L(j)	Sender is from Legal department, receiver is from Legal department
Ex2 = T(i)*L(j)	Sender is from Trading department, receiver is from Legal department
Ex3 = J(i)*L(j)	Sender's title is Junior, receiver is from Legal department
Ex4 = F(i)*L(j)	Sender is female, receiver is from Legal department
Ex5 = L(i)*T(j)	Sender is from Legal department, receiver is from Trading department
Ex6 = T(i)*T(j)	Sender is from Trading department, receiver is from Trading department
Ex7 = J(i)*T(j)	Sender's title is Junior, receiver is from Trading department
Ex8 = F(i)*T(j)	Sender is female, receiver is from Trading department
Ex9 = L(i)*J(j)	Sender is from Legal department, receiver's title is Junior
Ex10 = T(i)*J(j)	Sender is from Trading department, receiver's title is Junior
Ex11 = J(i)*J(j)	Sender's title is Junior, receiver's title is Junior
Ex12 = F(i)*J(j)	Sender is female, receiver's title is Junior
Ex13 = L(i)*F(j)	Sender is from Legal department, receiver is female
Ex14 = T(i)*F(j)	Sender is from Trading department, receiver is female
Ex15 = J(i)*F(j)	Sender's title is Junior, receiver is female
Ex16 = F(i)*F(j)	Sender is female, receiver is female
Same title	Sender and receiver has the same title
Same division	Sender and receiver are from the same company division

Table 3: List of effects for Enron Corpus data analysis, description of the exogenous events correspond to the covariate's value equal to one, and zero otherwise.

posterior distributions and 95% credible intervals are plotted in Figure 3. The credible intervals for the shrinkage models appear to be closer to zero, and the horseshoe often has a peak at zero. As expected, the flat prior model with no shrinkage returns the most significant predictors (fifteen); the ridge and the lasso model suggest fourteen significant predictors, and the horseshoe model results in the most parsimonious result with thirteen significant predictors (see Table 4).

Finally, we note that effects may not be identifiable for the flat prior model and the horseshoe model if there is not enough information in the data. In the analysis of the Enron data this problem occurred for 'Ex10', where the trajectory of the traceplot diverges. For the flat prior this can be caused by the prior being too 'vague' and the information in the effect not being enough for the posterior to detect. Similarly, the prior density of the horseshoe is less informative than for the ridge and lasso models, due to its thicker tails. To avoid this identification problem for effect 'Ex10', we excluded it from the estimation for the flat and horseshoe models.

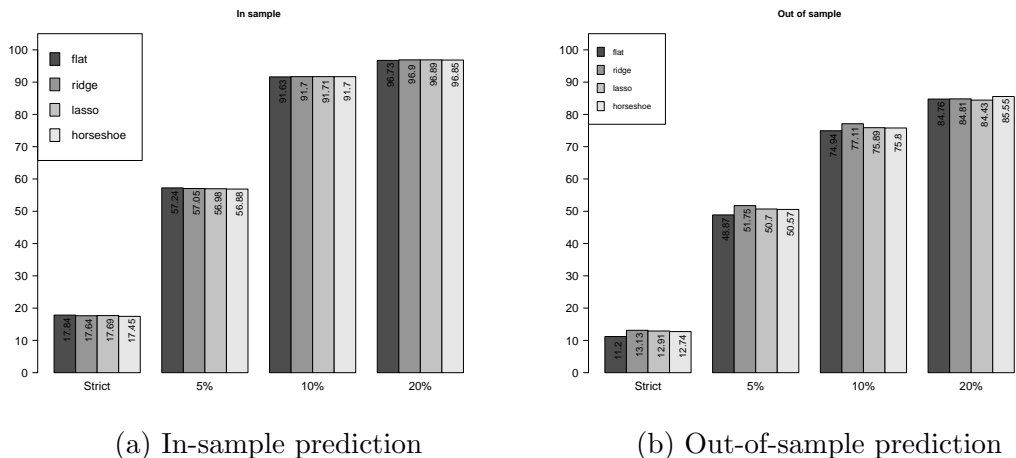


Figure 4: Prediction score measures based on posterior draws, in percentages, for the Enron data

Figure 4 reports the values of the posterior predictive measure for in sample prediction(6a) and out of sample prediction (6b) calculated for the next 1000 events in the sequence. In the case of in-sample prediction, when we count the number of predicted events exactly equal to the observed events, we find exactly predicted interactions in around 17% of the events, with the flat model having the highest score of 17.84%. In the 5% range, the flat model still gives the best performance (the observed interaction is among the top 5% predicted by the model in 57.2% of the events– while ridge, lasso and horseshoe have 57.1%, 57.0%, and 56.9% respectively. In both the top 10% and top

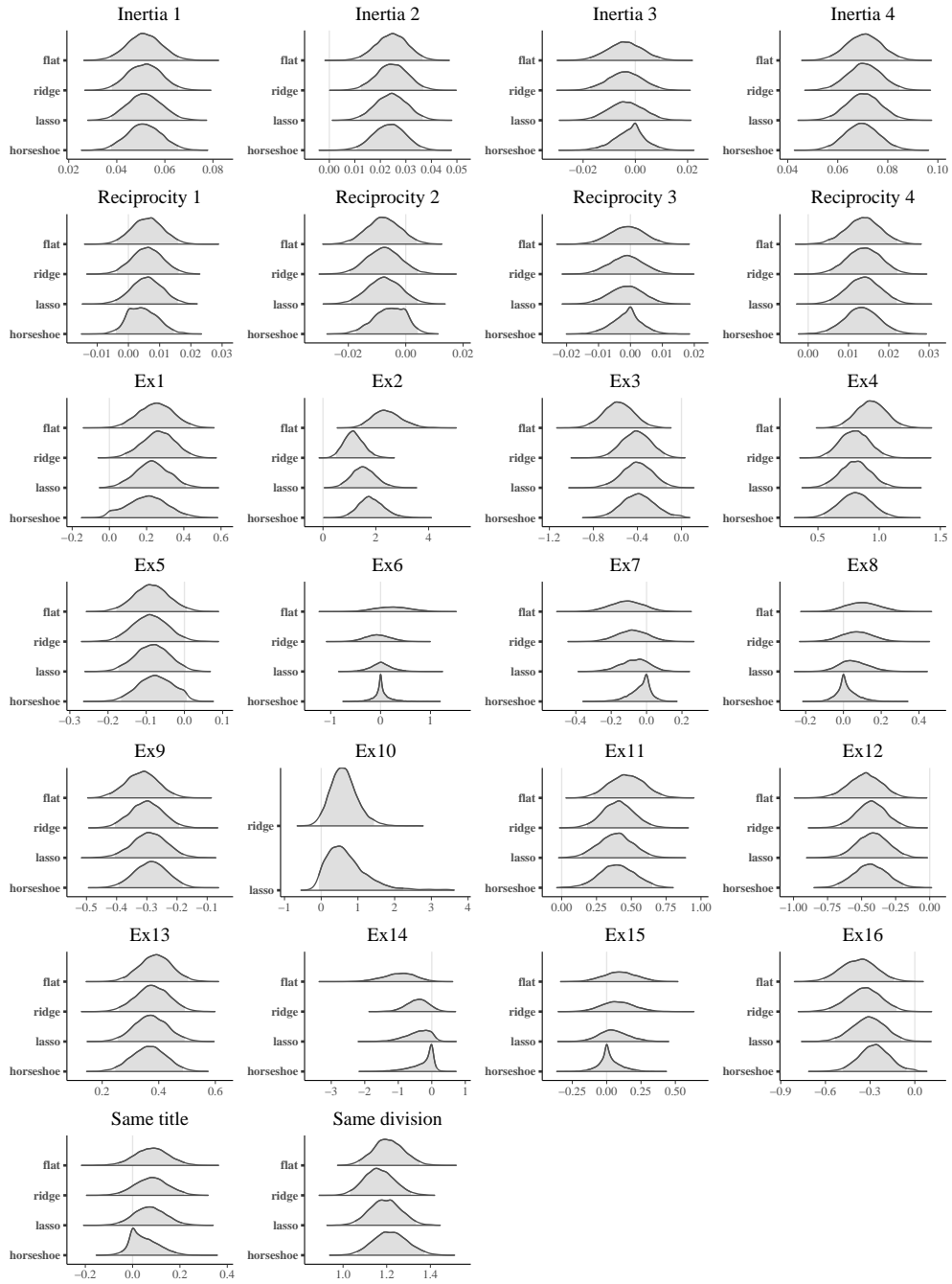


Figure 3: Density plots computed from posterior draws for Enron data estimation with 95% credible intervals shown as shaded areas under the curves.

20%, the shrinkage models perform (marginally) better than the no-shrinkage model. When considering out-of-sample prediction, where predictions were made for the next 1000 events, at least one shrinkage method shows higher scores than flat model in any score type.

4.1.1 Extended number of potential effects

As a further test of the performance of the shrinkage models, we run a simple simulation procedure to assess the Type I error rate. The aim of a shrinkage model is to separate the wheat from the chaff: statistics that do not have an effect on the observed event sequence should be recognized as not significant by these models. In this manner, the effects that are marked as significant are then indeed likely to really play a role in the social process that caused these events to occur. We can not know which of the statistics included in the model above truly did (not) affect the actual event sequence. Therefore, we could only check whether the shrinkage models would deliver predictive performance that is comparable to the non-shrinkage model, while potentially using fewer statistics. We now test whether the models can recognize statistics for which we know their true effect is zero. We explore the ability of the models to recognize such immaterial variables by generating 30 random covariates. Since we generated these ourselves, we know for a fact that they could not have caused any of the events in the event sequence. Hence, ideally, none of them should end up being significant in any model. We add these 30 fake covariates to the model and run the analyses again. The results are shown in Figure 5.

The flat prior model with no shrinkage effect marks 17 of the 55 effects (without ‘Ex10’) as significant, from which two effects are fake variables. For the ridge prior model, only one of the fake effects is significant, with the total number of fourteen significant covariates out of 56 considered. The lasso and horseshoe models eliminate all fake effects, which confirms the expected behavior of the shrinkage models, resulting in twelve and ten significant effects respectively. In addition, we see that the predictive performance score has increased (compared to the analysis without the fake covariates) as a result of overfitting by the flat prior model (see Figure 6) which is prevented by the shrinkage models. The shrinkage models (especially the lasso and horseshoe) do very well and separate the wheat from the chaff by shrinking the immaterial effects to zero, where the non-shrinkage model is fooled by some of them and reports two effects as significant of which we know for certain that they were unrelated to the observed event sequence.

Furthermore, we notice that adding more effects to the model can inflate the overall

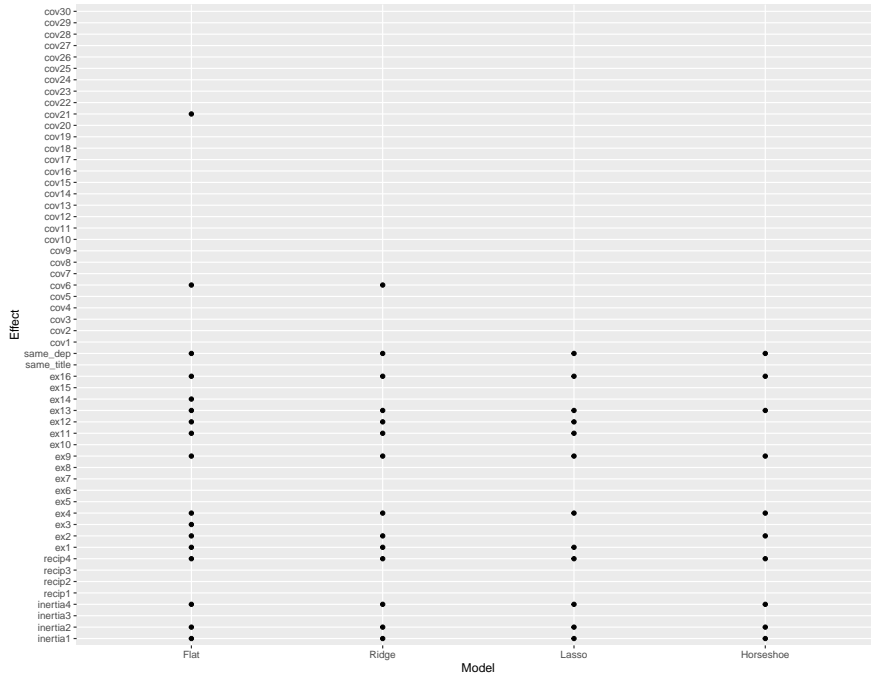
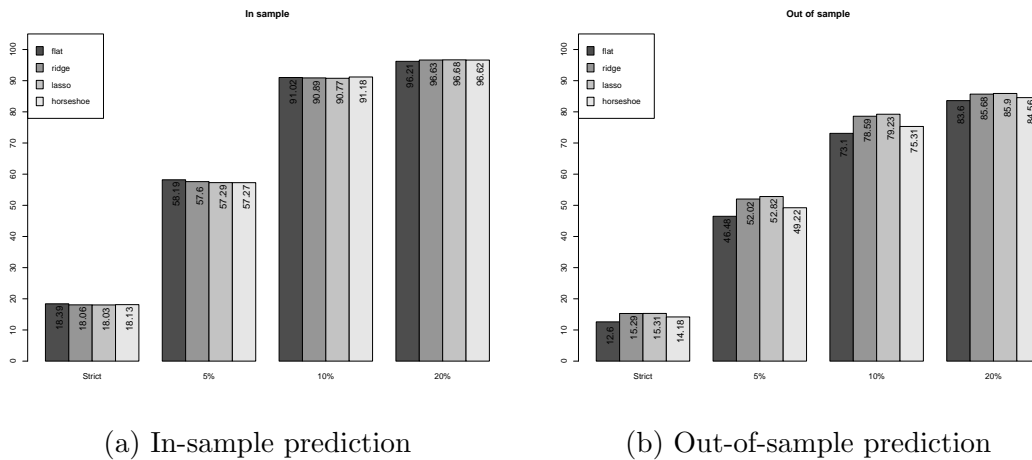


Figure 5: The resulting number of significant covariates based on credible intervals for Enron data



(a) In-sample prediction

(b) Out-of-sample prediction

Figure 6: Prediction score measures for the Enron data based on posterior draws, in percent (including the fake covariates)

shrinkage. For example, for the Enron data analysis lasso model detects fourteen predictors significant, while for the analysis with fake additional effects only twelve effects are significant. In the case of horseshoe model, these numbers are thirteen and ten respectively. More effects in the model can lead to larger sampled value of the shrinkage parameters, thus more effects are shrunk to zero.

4.2 Analyzing the Apollo 13 data using the dyadic model

In this section we analyse the Flight Director voice loops from the infamous Apollo 13 mission. The data were retrieved from <http://apollo13realtime.org/> and consist of recorded voice messages between sixteen members of the team. In the original data only the senders of the messages were recorded, we therefore added the receivers manually (based on the actual text of the messages). The event sequence includes 4239 messages within the time interval of the first six hours following the Apollo 13 accident. As the mission underwent different periods (e.g., after and before “Houston, we’ve had a problem”) the communication structure is likely to be different across these periods. This, again, suggests that the parameters of the relational event model likely change over time. Therefore we only consider the first 500 events which is a roughly stable period. For this data we estimate a dyad relational event model with 12 endogenous network effects: inertia, reciprocity, indegree, outdegree, and total degree for both sender and receiver, as well as participation shifts of the forms AB-BA, AB-BY, AB-XA, AB-AY (see Butts (2008) for the discussion of the network effects).

We estimated the four models on a subset of 500 first events using the Gibbs sampler algorithms described in Section 2 with 10000 iterations in burn-in period and total 10000 iterations, where only every tenth iteration is stored. The estimated posteriors and the 95% credible intervals are plotted in Figure 7. The differences between the posteriors of the four models are similar to those in the analysis of the Enron data. For the reciprocity statistic the flat no-shrinkage model does not include zero in the credible interval (neither does the ridge regression model). Alternatively, credible intervals for reciprocity in the lasso and horseshoe model do include zero, and for the horseshoe the probability mass is clearly concentrated at zero. The ridge prior model and the flat prior model each result in three significant effects. The horseshoe and lasso shrinkage models on the other hand eliminate the small negligible effect of reciprocity, resulting in two significant effects.

It is uncommon for a reciprocity effect to be zero in most social settings, especially in highly regulated situations as in a space flight. In fact, in our dataset, 259 events are sent and 234 are received by the flight director, mostly in back-and-forth interaction.

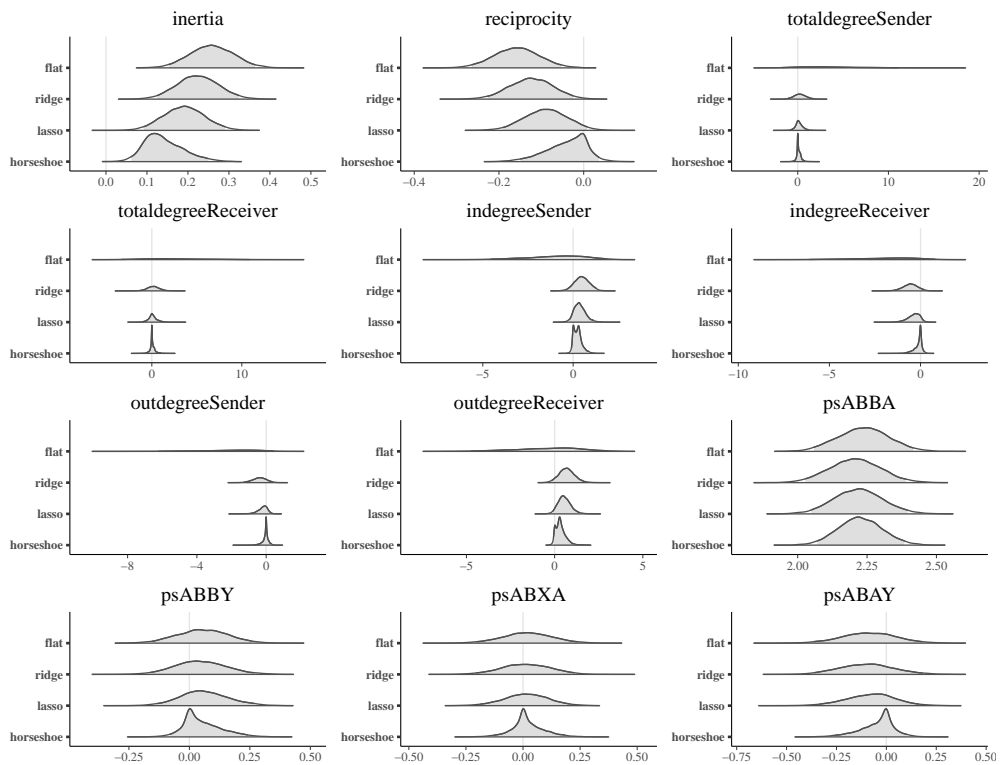


Figure 7: Posterior density plots and credible intervals for the Apollo 13 data.

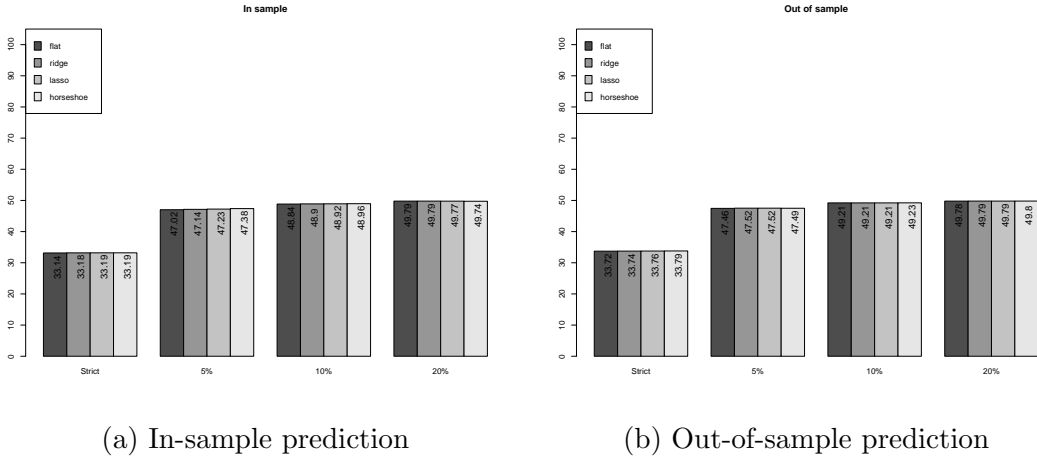


Figure 8: Prediction scores for the Apollo 13 data, in percent, based on posterior draws

This indicates an importance of the reciprocal behaviour for our dataset. Whereas the reciprocity statistic as defined by Butts (2008) captures a general trend towards interacting with past senders, the alternative statistic AB-BA captures *immediate* reciprocity: after A sends a message to B, B reciprocates this immediately. AB-BA statistic describes better the instant reciprocal behaviour in this data and has a large effect of around 2.25 that stays intact in the shrinkage models. In addition, we noticed that inertia and reciprocity statistics have a correlation of 0.97. Even with the presence of strong collinearity among the predictors, the lasso and horseshoe shrinkage models are able to eliminate the effect of reciprocity from the analysis.

Figure 8 reports the values of the posterior predictive measure for in sample prediction(8a) and out of sample prediction(8b). We see comparable predictive performance between the models, with marginal but constant improvement for the shrinkage methods compared to the flat prior model. The same observation holds for the out-of-sample prediction. The shrinkage models do this with more parsimonious and more easily interpreted models. While the shrinkage model eliminated a negligible effect of reciprocity statistic, the prediction score for shrinkage models does not decrease much compared to the one for flat model.

4.2.1 Extended number of potential effects

The statistics that are found to be significant in the models make great substantive sense and would be expected to be found for an interaction sequence as a space flight. We now extend the dataset by adding randomly generated (fake) statistics to the model,

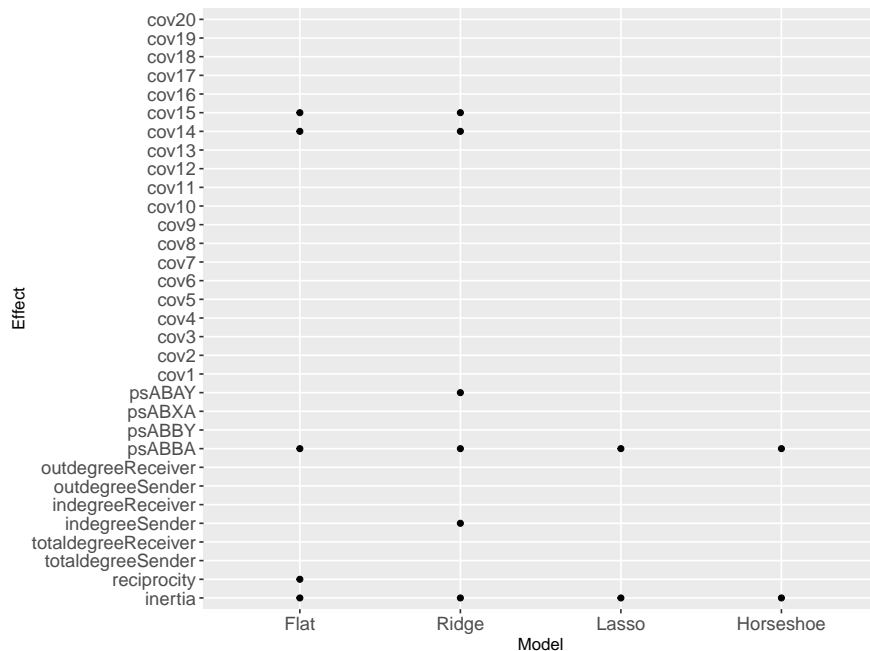
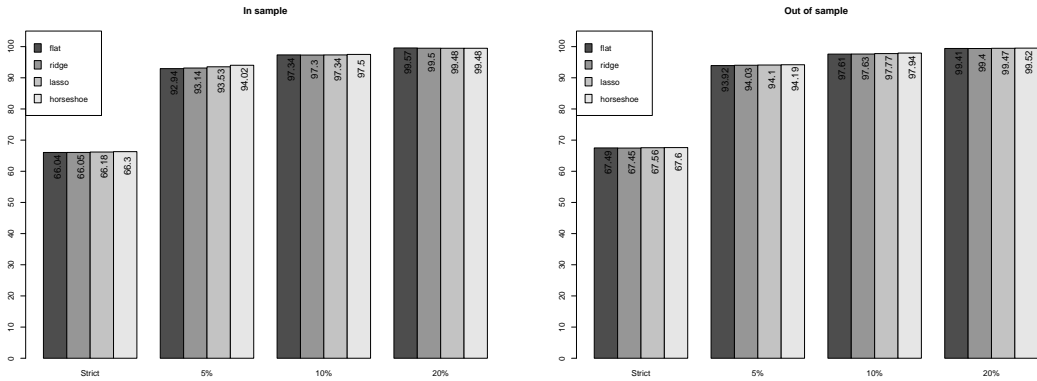


Figure 9: The resulting number of significant covariates for the Apollo 13 data

similarly to the analysis of the Enron data in Section 4.1. Figure 9 displays which effects are considered significant by each of the models, based on the 95% credible intervals. The flat and ridge models mark two of the fake covariates as significant, while lasso and horseshoe models with stronger shrinkage effect are not tricked and do not mark any of the fake covariates as significant resulting in a parsimonious and more correct model.

Figure 10 reports the values of the posterior predictive measures for in-sample prediction(10a) and out-of-sample prediction(10b) based on the models with the full data sets (including the fake covariates). The scores are considerably higher than for the primary analysis without the additional fake covariates; this supports the hypothesis that the shrinkage models do perform better in the case of sparse effects. In both in-sample and out-of-sample cases, the no shrinkage model has the lowest performance in almost in all cases. Among the shrinkage models, the horseshoe and lasso models slightly outperform the ridge regression model. We conclude that the shrinkage models were able to recognize the fake statistics as unconnected to the data generation process. As a result, they are less prone to overfitting or to added noise induced by irrelevant predictors.



(a) In-sample prediction

(b) Out-of-sample prediction

Figure 10: Prediction score measures for the Apollo 13 data, in percent, based on posterior draws (including the fake covariates)

5 Discussion

The scope of this paper was to extend Bayesian variable selection methods to relational event data analyses. Recent research shows that the evolution of relational event networks and the formation of the links between actors can be triggered by a great variety of (complex) effects (both endogenous network effects and exogenous statistics, as well as interaction effects). Therefore, there is a need for statistical algorithms that are able to separate the wheat from the chaff to recognize the true nonzero effects. This results in the more parsimonious relational event models that are easier to interpret and have good predictive performance. The proposed Bayesian shrinkage models provide an effective solution to this problem.

The Bayesian shrinkage methods show promising results in detecting relevant predictors without sacrificing predictive accuracy (and in some cases even improving prediction accuracy). Furthermore, by considering a full Bayesian approach, the shrinkage parameter is jointly estimated with the other model parameters, and thus no (ad hoc) cross-validation methods are needed to determine the shrinkage parameters as would be the case in a non-Bayesian penalized regression. Moreover, we obtain a clear Bayesian interpretation of the results where parameter uncertainty is naturally incorporated – this is not the case with the classical lasso which may, in turn, result in standard errors of zero. A further advantage of shrinkage priors is that they can avoid identification issues and guarantee convergence of the Gibbs sampler.

When prior information about the possible distribution of effects is not available, our recommendation is to use all three models discussed in this paper and compare their

posterior predictive measures afterwards. The horseshoe prior generally results in the most parsimonious model because it can have zeros as the point estimates (posterior modes). This tends to lead to the model that is the easiest to interpret with effects that are the least likely to be significant “by accident”. This makes the final modeling more conservative, which is probably a good thing considering that there is little (if any) solid theory to base the choice of predictors in relational event models on.

Our study suggests that adding a large number of predictors in the model may lead to a magnified shrinkage effect. This can be explained by the fact that the shrinkage parameter is optimized based on all the predictors in the model. Thus, if more variables that are added have an approximate zero effect, the average degree of shrinkage of all effects will be slightly larger. If, on the other hand, variables would be added with relatively large, nonzero effects, the average degree of shrinkage of all effects will be slightly smaller. Note that a similar behavior would be observed in classical regularization methods. As a possible remedy, one can define separate shrinkage priors for different sets of the effects in the model to control the average amount of shrinkage differently across these different sets. This would be an interesting extension for future work on Bayesian regularization of relational event models. A further study could assess the possible benefits of such fine-grained shrinkage methods.

In addition, further research can explore the use of shrinkage priors to model temporal changes of network parameters over time. The idea would be to place a shrinkage prior for the difference of a parameter over time, similar as in graphical models for variables (Shafiee Kamalabad and Grzegorzcyk, 2020). When the parameter is approximately constant over time, the difference is shrunk to zero such that the estimated parameter remains constant. If the parameter does change, e.g., due to a switch between interaction regimes between the actors, no shrinkage should be applied and we would be able to identify a change of the interaction regime in the network.

A Tables and graphs

Effect	Models			
	Flat	Ridge	Lasso	Horseshoe
Inertia 1	(0.0374, 0.0655)	(0.0379, 0.0655)	(0.0378, 0.0657)	(0.0375, 0.0656)
Inertia 2	(0.012, 0.0365)	(0.0124, 0.0368)	(0.012, 0.0366)	(0.0108, 0.0357)
Inertia 3	(-0.0174, 0.0093)	(-0.0173, 0.0089)	(-0.0168, 0.0093)	(-0.0152, 0.0093)
Inertia 4	(0.0568, 0.0843)	(0.057, 0.0846)	(0.0568, 0.084)	(0.056, 0.0834)
Reciprocity 1	(-0.0038, 0.0159)	(-0.0037, 0.0161)	(-0.0042, 0.0158)	(-0.004, 0.0145)
Reciprocity 2	(-0.0195, 0.0038)	(-0.0195, 0.0042)	(-0.0191, 0.0041)	(-0.0173, 0.0042)
Reciprocity 3	(-0.0118, 0.0093)	(-0.0118, 0.0091)	(-0.0119, 0.009)	(-0.0109, 0.0078)
Reciprocity 4	(0.005, 0.0221)	(0.0054, 0.0221)	(0.0054, 0.022)	(0.0046, 0.0219)
Ex1	(0.0651, 0.4367)	(0.0864, 0.4342)	(0.0532, 0.4113)	(-0.0003, 0.4175)
Ex2	(1.4358, 3.5986)	(0.491, 1.9644)	(0.6754, 2.5357)	(0.9374, 2.8983)
Ex3	(-0.8426, -0.305)	(-0.6689, -0.1522)	(-0.6878, -0.1317)	(-0.6775, -0.066)
Ex4	(0.6988, 1.1809)	(0.5721, 1.0373)	(0.5611, 1.0591)	(0.549, 1.0691)
Ex5	(-0.1782, 0.0065)	(-0.1806, 0.002)	(-0.1727, 0.003)	(-0.1659, 0.0059)
Ex6	(-0.4597, 0.9358)	(-0.5537, 0.4543)	(-0.458, 0.504)	(-0.3299, 0.4403)
Ex7	(-0.3, 0.0733)	(-0.2553, 0.0976)	(-0.2432, 0.0894)	(-0.1801, 0.0674)
Ex8	(-0.0706, 0.2764)	(-0.0986, 0.2387)	(-0.09, 0.2231)	(-0.0832, 0.1472)
Ex9	(-0.4247, -0.2086)	(-0.4057, -0.1937)	(-0.4057, -0.1787)	(-0.3939, -0.1817)
Ex10		(-0.0331, 1.4379)	(-0.0648, 2.2296)	
Ex11	(0.2266, 0.714)	(0.1825, 0.6399)	(0.1455, 0.6281)	(0.1454, 0.6501)
Ex12	(-0.7198, -0.2434)	(-0.6555, -0.2116)	(-0.6547, -0.1912)	(-0.6751, -0.1962)
Ex13	(0.2737, 0.5034)	(0.2596, 0.4921)	(0.2556, 0.4913)	(0.2463, 0.4853)
Ex14	(-2.0284, -0.0974)	(-1.1362, 0.1878)	(-1.3042, 0.1454)	(-1.2347, 0.1396)
Ex15	(-0.1411, 0.3399)	(-0.1496, 0.3241)	(-0.1534, 0.2769)	(-0.1395, 0.2143)
Ex16	(-0.6111, -0.1409)	(-0.576, -0.1227)	(-0.5362, -0.0911)	(-0.4818, -0.0565)
Same title	(-0.0617, 0.2192)	(-0.0593, 0.2171)	(-0.0574, 0.2074)	(-0.0488, 0.1832)
Same division	(1.0716, 1.3499)	(1.0323, 1.3105)	(1.0565, 1.3337)	(1.0664, 1.3732)
Number of significant covariates	15	14	14	13

Table 4: 95% Credible intervals for the Enron corpus data.

	First analysis				Extended analysis			
	Flat	Ridge	Lasso	Horseshoe	Flat	Ridge	Lasso	Horseshoe
Inertia 1	0.05	0.052	0.052	0.05	0.055	0.053	0.053	0.052
Inertia 2	0.024	0.023	0.024	0.021	0.024	0.026	0.026	0.022
Inertia 3	-0.003	-0.003	-0.002	0	-0.004	-0.004	-0.005	0
Inertia 4	0.072	0.07	0.072	0.068	0.07	0.071	0.068	0.067
Reciprocity 1	0.007	0.006	0.006	0	0.006	0.005	0.005	0
Reciprocity 2	-0.009	-0.007	-0.008	0	-0.007	-0.008	-0.008	0
Reciprocity 3	0	0	-0.002	0	-0.001	0	-0.001	0
Reciprocity 4	0.013	0.013	0.014	0.014	0.014	0.014	0.014	0.013
Ex1	0.248	0.256	0.219	0.205	0.264	0.348	0.223	0
Ex2	2.341	1.19	1.551	1.723	2.211	0.555	0.418	1.604
Ex3	-0.605	-0.433	-0.42	-0.403	-0.564	-0.213	-0.113	-0.001
Ex4	0.912	0.808	0.77	0.837	0.913	0.636	0.61	0.735
Ex5	-0.09	-0.094	-0.09	-0.076	-0.054	-0.037	-0.032	0
Ex6	0.276	-0.101	0.005	0	0.319	-0.091	-0.008	-0.001
Ex7	-0.104	-0.095	-0.044	-0.001	-0.125	-0.032	-0.024	0
Ex8	0.113	0.074	0.029	0	0.171	0.055	-0.001	0
Ex9	-0.313	-0.297	-0.286	-0.274	-0.323	-0.293	-0.259	-0.275
Ex10		0.602	0.482			0.27	0.008	
Ex11	0.449	0.398	0.418	0.385	0.456	0.358	0.257	-0.001
Ex12	-0.468	-0.422	-0.388	-0.409	-0.513	-0.381	-0.355	0.001
Ex13	0.392	0.379	0.373	0.356	0.393	0.356	0.356	0.346
Ex14	-0.805	-0.416	-0.168	-0.002	-0.896	-0.094	-0.008	0
Ex15	0.143	0.044	0.025	0.001	0.113	0.035	0.003	0
Ex16	-0.356	-0.314	-0.319	-0.284	-0.382	-0.246	-0.213	-0.273
Same title	0.09	0.086	0.088	0	0.077	0.077	0.06	0
Same division	1.169	1.163	1.22	1.189	1.194	1.099	1.178	1.295
Cov1					0.011	0.013	0.01	0
Cov2					-0.026	-0.026	-0.019	0
Cov3					0.01	0.011	0.008	0
Cov4					-0.025	-0.019	-0.01	0
Cov5					0.003	0.004	0.008	0
Cov6					-0.048	-0.052	-0.033	0
Cov7					-0.007	-0.004	-0.002	0
Cov8					-0.02	-0.044	-0.016	0
Cov9					-0.047	-0.065	-0.041	0
Cov10					-0.004	0	0.003	0
Cov11					0	-0.001	0	0
Cov12					-0.008	-0.007	-0.002	0
Cov13					-0.02	-0.028	-0.026	0
Cov14					-0.003	-0.004	-0.003	0
Cov15					-0.005	-0.007	-0.002	0
Cov16					0.018	0.016	0.008	0
Cov17					-0.001	0	-0.001	0
Cov18					0.002	-0.005	-0.002	0
Cov19					-0.005	-0.001	0	0
Cov20					-0.057	-0.059	-0.049	0
Cov21					-0.056	-0.05	-0.045	0
Cov22					-0.012	-0.007	-0.001	0
Cov23					0.052	0.038	0.034	0
Cov24					-0.038	-0.025	-0.024	0
Cov25					-0.017	-0.009	-0.019	0
Cov26					-0.004	-0.002	0.005	0
Cov27					-0.025	-0.022	-0.018	0
Cov28					-0.029	-0.034	-0.024	0
Cov29					-0.023	-0.02	-0.012	0
Cov30					-0.001	0.009	-0.006	0

Table 5: Values of the posterior mode, for effects in primary and extended model of the Enron data.

Effect	Models			
	Flat	Ridge	Lasso	Horseshoe
inertia	(0.1534, 0.3637)	(0.1252, 0.3245)	(0.092, 0.2903)	(0.0619, 0.2493)
reciprocity	(-0.2639, -0.0532)	(-0.2268, -0.0248)	(-0.1903, 0.008)	(-0.1487, 0.0359)
totaldegreeSender	(-1.7193, 11.0226)	(-1.0695, 1.6201)	(-0.7217, 1.1752)	(-0.4284, 0.7854)
totaldegreeReceiver	(-3.387, 10.8856)	(-1.2338, 1.5439)	(-0.9548, 1.2621)	(-0.6525, 0.9483)
indegreeSender	(-4.551, 1.8027)	(-0.3251, 1.2836)	(-0.2205, 1.1097)	(-0.0923, 0.8393)
indegreeReceiver	(-6.1018, 0.7916)	(-1.4129, 0.1896)	(-1.1552, 0.1747)	(-0.8213, 0.1979)
outdegreeSender	(-6.2074, 0.4214)	(-1.2295, 0.3718)	(-0.905, 0.283)	(-0.6009, 0.2843)
outdegreeReceiver	(-4.7354, 2.9554)	(-0.1644, 1.6278)	(-0.1012, 1.3676)	(-0.0604, 1.094)
psABBA	(2.0586, 2.4161)	(2.028, 2.3898)	(2.0491, 2.3957)	(2.0709, 2.3846)
psABBY	(-0.1529, 0.2578)	(-0.1614, 0.2665)	(-0.1319, 0.2683)	(-0.0798, 0.2405)
psABXA	(-0.2021, 0.2382)	(-0.2035, 0.2223)	(-0.1854, 0.2056)	(-0.1269, 0.1815)
psABAY	(-0.3606, 0.178)	(-0.3595, 0.1787)	(-0.3332, 0.1615)	(-0.2548, 0.1026)
Number of significant covariates	3	3	2	2

Table 6: Credible intervals for the Apollo 13 data

	First analysis				Extended analysis			
	Flat	Ridge	Lasso	Horseshoe	Flat	Ridge	Lasso	Horseshoe
inertia	0.255	0.222	0.196	0.104	0.231	0.15	0.113	0.094
reciprocity	-0.161	-0.122	-0.082	0	-0.148	-0.085	-0.037	0
totaldegreeSender	3.017	0.256	0.004	-0.002	1.11	0.173	0.002	-0.001
totaldegreeReceiver	1.092	0.326	-0.004	0.004	2.007	0.291	0.002	0
indegreeSender	-0.537	0.389	0.345	0.002	0.388	0.537	0.344	0.001
indegreeReceiver	-0.905	-0.591	-0.289	-0.002	-1.007	-0.092	-0.003	0
outdegreeSender	-1.502	-0.319	-0.111	-0.001	-0.8	-0.262	0	-0.001
outdegreeReceiver	0.598	0.675	0.456	0.003	0.266	0.37	0.224	0
psABBA	2.23	2.203	2.225	2.227	2.145	2.067	2.167	2.218
psABBY	0.044	0.022	0.049	0	-0.073	-0.086	-0.001	0
psABXA	0.026	0.014	0	0	-0.095	-0.104	-0.024	0
psABAY	-0.099	-0.103	-0.052	0.001	-0.232	-0.302	-0.123	-0.001
cov1					-0.035	-0.023	-0.009	0
cov2					0.013	0.015	0.011	0
cov3					-0.04	-0.027	-0.007	0
cov4					0.023	0.014	0.012	0
cov5					-0.022	-0.004	-0.018	0
cov6					-0.008	-0.002	0.009	0
cov7					-0.021	-0.014	-0.011	0
cov8					-0.046	-0.04	-0.036	0
cov9					-0.034	-0.029	-0.015	0
cov10					-0.02	-0.024	-0.02	0
cov11					-0.124	-0.114	-0.094	0
cov12					-0.151	-0.128	-0.102	0
cov13					-0.003	-0.024	-0.01	0
cov14					-0.212	-0.222	-0.165	0
cov15					-0.223	-0.188	-0.15	0
cov16					-0.126	-0.131	-0.123	0
cov17					-0.111	-0.049	-0.01	0
cov18					-0.103	-0.097	-0.073	0
cov19					-0.096	-0.124	-0.039	0
cov20					-0.201	-0.153	-0.123	-0.001

Table 7: Posterior mode values for the Apollo 13 mission analysis

References

- Albert, J. H. and Chib, S. (1993). Bayesian analysis of binary and polychotomous response data. *Journal of the American statistical Association*, 88(422):669–679.
- Arena, G., Mulder, J., and Leenders, R. T. A. J. (2021). A Bayesian semi-parametric approach for modeling memory decay in dynamic social networks. [<https://arxiv.org/abs/2109.01881>].
- Bhadra, A., Datta, J., Polson, N. G., Willard, B., et al. (2019). Lasso meets horseshoe: A survey. *Statistical Science*, 34(3):405–427.
- Brandes, U., Lerner, J., and Snijders, T. A. (2009). Networks evolving step by step: Statistical analysis of dyadic event data. In *2009 international conference on advances in Social network analysis and mining*, pages 200–205. IEEE.
- Butts, C. T. (2008). A Relational Event Framework for Social Action. *Sociological Methodology*, 38(1):155–200.
- Carvalho, C. M., Polson, N. G., and Scott, J. G. (2009). Handling sparsity via the horseshoe. In *Artificial Intelligence and Statistics*, pages 73–80.
- Carvalho, C. M., Polson, N. G., and Scott, J. G. (2010). The horseshoe estimator for sparse signals. *Biometrika*, 97(2):465–480.
- Chib, S. and Greenberg, E. (1998). Analysis of multivariate probit models. *Biometrika*, 85(2):347–361.
- Cox, D. R. (1972). Regression models and life-tables. *Journal of the Royal Statistical Society: Series B (Methodological)*, 34(2):187–202.
- Diesner, J., Frantz, T. L., and Carley, K. M. (2005). Communication networks from the enron email corpus “it’s always about the people. enron is no different”. *Computational & Mathematical Organization Theory*, 11(3):201–228.
- DuBois, C., Butts, C. T., McFarland, D., and Smyth, P. (2013). Hierarchical models for relational event sequences. *Journal of Mathematical Psychology*, 57(6):297–309.
- Frühwirth-Schnatter, S. and Frühwirth, R. (2012). Bayesian inference in the multinomial logit model. *Austrian Journal of Statistics*, 41(1):27–43.

- Gelman, A., Carlin, J. B., Stern, H. S., Dunson, D. B., Vehtari, A., and Rubin, D. B. (2013). *Bayesian data analysis*. CRC press.
- Gumbel, E. J. (1961). Bivariate logistic distributions. *Journal of the American Statistical Association*, 56(294):335–349.
- Hedström, P. and Bearman, P. (2009). What is analytical sociology all about? an introductory essay. *The Oxford handbook of analytical sociology*, pages 3–24.
- Hoffman, M., Block, P., Elmer, T., and Stadtfeld, C. (2020). A model for the dynamics of face-to-face interactions in social groups. *Network Science*, 8(S1):S4–S25.
- Holmes, C. C., Held, L., et al. (2006). Bayesian auxiliary variable models for binary and multinomial regression. *Bayesian analysis*, 1(1):145–168.
- Imai, K. and Van Dyk, D. A. (2005). A Bayesian analysis of the multinomial probit model using marginal data augmentation. *Journal of econometrics*, 124(2):311–334.
- Keila, P. S. and Skillicorn, D. B. (2005). Structure in the enron email dataset. *Computational & Mathematical Organization Theory*, 11(3):183–199.
- Kyung, M., Gill, J., Ghosh, M., Casella, G., et al. (2010). Penalized regression, standard errors, and bayesian lassos. *Bayesian Analysis*, 5(2):369–411.
- Leenders, R. T. A., Contractor, N. S., and DeChurch, L. A. (2016). Once upon a time: Understanding team processes as relational event networks. *Organizational Psychology Review*, 6(1):92–115.
- Lerner, J. and Lomi, A. (2018). Let’s talk about refugees: Network effects drive contributor attention to wikipedia articles about migration-related topics. In *International Conference on Complex Networks and their Applications*, pages 211–222. Springer.
- Lerner, J. and Lomi, A. (2020). Reliability of relational event model estimates under sampling: How to fit a relational event model to 360 million dyadic events. *Network Science*, 8(1):97–135.
- Liang, H. (2014). The organizational principles of online political discussion: A relational event stream model for analysis of web forum deliberation. *Human Communication Research*, 40(4):483–507.
- Malang, T., Brandenberger, L., and Leifeld, P. (2019). Networks and social influence in european legislative politics. *British Journal of Political Science*, 49(4):1475–1498.

- Malik, H. J., Abraham, B., et al. (1973). Multivariate logistic distributions. *The Annals of Statistics*, 1(3):588–590.
- Mulder, J. and Leenders, R. T. A. (2019). Modeling the evolution of interaction behavior in social networks: A dynamic relational event approach for real-time analysis. *Chaos, Solitons & Fractals*, 119:73–85.
- Mulder, J., Pericchi, L. R., et al. (2018). The matrix- f prior for estimating and testing covariance matrices. *Bayesian Analysis*, 13(4):1193–1214.
- O’Brien, S. M. and Dunson, D. B. (2004). Bayesian multivariate logistic regression. *Biometrics*, 60(3):739–746.
- Park, T. and Casella, G. (2008). The Bayesian Lasso. *Journal of the American Statistical Association*, 103(482):681–686.
- Perry, P. O. and Wolfe, P. J. (2013). Point process modelling for directed interaction networks. *Journal of the Royal Statistical Society: Series B (Statistical Methodology)*, 75(5):821–849.
- Peterson, K., Hohensee, M., and Xia, F. (2011). Email formality in the workplace: A case study on the enron corpus. In *Proceedings of the Workshop on Language in Social Media (LSM 2011)*, pages 86–95.
- Pilny, A., Schechter, A., Poole, M. S., and Contractor, N. (2016). An illustration of the relational event model to analyze group interaction processes. *Group Dynamics: Theory, Research, and Practice*, 20(3):181.
- Quintane, E., Conaldi, G., Tonellato, M., and Lomi, A. (2014). Modeling relational events: A case study on an open source software project. *Organizational Research Methods*, 17(1):23–50.
- Shafiee Kamalabad, M. and Grzegorzczak, M. (2020). Non-homogeneous dynamic bayesian networks with edge-wise sequentially coupled parameters. *Bioinformatics*, 36(4):1198–1207.
- Snijders, T. A. B. (2005). Models for longitudinal network data. *Models and Methods in Social Network Analysis*, 1:215–247.
- Stadtfeld, C. and Block, P. (2017). Interactions, actors, and time: Dynamic network actor models for relational events. *Sociological Science*, 4:318–352.

- Stadtfeld, C., Hollway, J., and Block, P. (2017). Dynamic Network Actor Models: Investigating coordination ties through time. *Sociological Methodology*, 47(1):1–40.
- Tibshirani, R. (1996). Regression shrinkage and selection via the lasso. *Journal of the Royal Statistical Society: Series B (Methodological)*, 58(1):267–288.
- Van Erp, S., Oberski, D. L., and Mulder, J. (2019). Shrinkage priors for bayesian penalized regression. *Journal of Mathematical Psychology*, 89:31–50.
- Vu, D., Lomi, A., Mascia, D., and Pallotti, F. (2017). Relational event models for longitudinal network data with an application to interhospital patient transfers. *Statistics in medicine*, 36(14):2265–2287.
- Wilson, G. and Banzhaf, W. (2009). Discovery of email communication networks from the enron corpus with a genetic algorithm using social network analysis. In *2009 IEEE Congress on Evolutionary Computation*, pages 3256–3263.
- Zhou, Y., Goldberg, M., Magdon-Ismail, M., and Wallace, A. (2007). Strategies for cleaning organizational emails with an application to enron email dataset. In *5th Conf. of North American Association for Computational Social and Organizational Science*, number 0621303.